

Persistence of phase boundaries between a topological and trivial Z_2 insulator.

Zohar Ringel and Ehud Altman

Department of Condensed Matter Physics, Weizmann Institute of Science, Rehovot 76100, Israel

When time reversal symmetry is present there is a sharp distinction between topological and trivial band insulators which ensures that, as parameters are varied, these phases are separated by a phase transition at which the bulk gap closes. Surprisingly we find that even in the absence of time reversal symmetry, gapless regions originating from the phase boundaries persist. Moreover the critical line generically opens up to enclose Chern insulating phases that are thin but of finite extent in the phase diagram. We explain the topological origin of this effect in terms of quantized charge pumping, showing in particular that it is robust to the effect of disorder and interactions.

PACS numbers: 73.43.-f, 73.43.Cd, 71.23.-k, 71.10.Fd

I. INTRODUCTION

The distinction between Topological and ordinary band insulators relies on time reversal symmetry (TRS)^{1,2}. In the presence of this symmetry the two phases must be separated in parameter space by a quantum phase transition at which the energy gap vanishes. Similarly a real space boundary between the two insulators must sustain protected metallic edge states, as has been clearly observed in experiment^{3,4}. When time reversal symmetry (TRS) is broken the edge states generally become gapped or localized by disorder⁵, albeit some residual consequences of the bulk topology, such as a surface Chern number, may remain. Because there is at least a superficial relation between the edge states in real space and the gapless (critical) phase boundaries in parameter space, it is natural to ask what is the fate of the latter when time reversal symmetry is broken. Are these critical regions in the phase diagram immediately gapped out or localized, or do they contain some robust features that are not destroyed by the symmetry breaking?

In this paper we assess the robustness of the critical lines that enclose a $2D$ topological insulator in parameter space, separating it from an ordinary band insulator. We first derive general criteria for stability of those critical regions to weak TRS breaking perturbations. We further show that in certain cases the critical regions have a stronger topological protection, which does not rely on time reversal symmetry and is hence much stronger than the protection of the gapped insulators. In this case the gapless surface that enclosed the topological phase in parameter space may split up into segments to allow adiabatic connection between the former topological and ordinary insulators. However, the critical segments persist and cannot terminate for arbitrarily strong symmetry breaking perturbations.

For a two dimensional non interacting and translational invariant model, the topological criterion can be simply formulated in terms of a winding number on the Brillouin zone. The critical point between a topological and ordinary band insulator is where the bulk Dirac dispersion becomes massless. These gapless points follow a certain trajectory in k -space as the parameters are varied

along a critical line that encloses the topological insulator in the phase diagram. We assert that the critical regions persist for arbitrary time reversal symmetry breaking, if the trajectory of Dirac points winds around the Brillouin zone.

To establish the robustness of the critical region also in presence of disorder and interactions we make a connection between the winding number on the Brillouin zone and a Chern number associated with charge pumping. Specifically the winding of the Dirac points on the Brillouin zone is directly related to a Chern number defined on a path in parameter space that encircles the topological phase from the outside, i.e. on a path that lies entirely in the ordinary insulating phase. A non zero Chern number implies pumping of an integer number of particles per row of the lattice upon following such a closed adiabatic path. Hence, the critical phase boundary might exhibit a topological protection that is much stronger than that of the insulating phases⁶. In contrast to the latter, this topological protection does not rely on time reversal symmetry but only on particle number conservation.

II. ROBUST CRITICAL REGIONS IN AN EXTENDED KANE AND MELE MODEL

To elucidate the main results of the paper we first demonstrate the aforementioned features on a concrete $2D$ tight binding model which can be tuned between a topological insulator (TI) and a band insulator (BI). This model is an extension of the Kane and Mele model¹, describing electrons hopping on a Honeycomb lattice in the presence of spin-orbit coupling. It includes two parameters, staggered hopping and staggered potential, which drive the system into a BI phase. As a function of these, the phase diagram consists of an elliptical TI region encircled by a BI phase with a critical line in between. We shall study the fate of this line as TRS is broken by a staggered and a uniform in-plane Zeeman field.

The corresponding Hamiltonian is given by

$$\begin{aligned}
\mathbf{H}_{\text{km}} &= \mathbf{H}_{\text{g}} + \mathbf{V}_{\text{so}} + \mathbf{V}_{\text{stag}} + \mathbf{V}_{\text{so}} + \mathbf{V}_{\delta t}, \quad (1) \\
\mathbf{H}_{\text{g}} &= \sum_{\langle ij \rangle, s} t c_{is}^\dagger c_{js}, \\
\mathbf{V}_{\text{sta}} &= \Delta \sum_{is} \xi_i c_{is}^\dagger c_{is}, \\
\mathbf{V}_{\text{so}} &= i\lambda_{so} \sum_{\langle\langle ij \rangle\rangle, s} \nu_{ij} s c_{is}^\dagger c_{js} \\
&\quad + i\lambda_R \sum_{\langle ij \rangle} c_{is}^\dagger (\vec{\sigma}_{ss'} \times \hat{d}_{ij})_z c_{js'}, \\
\mathbf{V}_{\delta t} &= \delta t \sum_{i-j=\pm d_3} c_{is}^\dagger (1 + s\lambda_R/t) c_{js} \\
&\quad - \delta t \sum_{i-j=\pm d_2} c_{is}^\dagger (1 - s\lambda_R/t) c_{js},
\end{aligned}$$

Here c_{is} annihilates an electron with $S_z = s$ on the i 'th site of an hexagonal lattice, $\xi_i = \pm 1$ is an alternating sign on the two sublattices, $\langle\langle ij \rangle\rangle$ denotes next-nearest-neighbor sites and $\nu_{i,j} = 1(-1)$ if the lattice path between the two sites i and j , winds clock-wise (counter clock-wise). The vectors d_i and the staggered hopping pattern are shown in Fig. (1). Summation of repeated indices is implicit. Notably the model includes an extra Rashba term proportional to δt , that couples to the out-of-plane spin component. The reason for adding the additional spin orbit term is to break spurious symmetries⁷ of the model and thus explore generic features.

In the absence of TRS breaking perturbations, the phase diagram of the above model in the plane of $(\Delta, \delta t)$ consists of an inner TI phase separated by a critical line from an outer BI phase, as shown in Fig. (2a), dashed red line. To test the robustness of this line we consider a staggered (M_{stg}) and uniform (M_x) Zeeman field terms in the x -direction

$$\begin{aligned}
\mathbf{V}_{\text{M}} &= M_{\text{stg}} \sum_i \xi_i c_{i,\sigma}^\dagger [\sigma_x]_{\sigma,\sigma'} c_{i,\sigma'} \quad (2) \\
&\quad + M_x \sum_i c_{i,\sigma}^\dagger [\sigma_x]_{\sigma,\sigma'} c_{i,\sigma'}
\end{aligned}$$

The staggered term may arise if the system breaks TRS spontaneously by developing an in-plane anti-ferromagnetic order. We have verified that strong Hubbard-type repulsive interactions indeed lead to such a symmetry breaking with an in-plane magnetization (see also⁸).

Figure (2) shows the numerically obtained phase diagram in $(\Delta, \delta t)$ plane for different TRS breaking perturbations and fixed values of the remaining parameters ($t = 1, \lambda_{so} = 1$ and $\lambda_R = 0.5$). Fig. (2 a) and (2 b), show the phase diagram for non-zero staggered field ($M_{\text{stg}} = 2$) and non-zero uniform field ($M_x = 0.5$), respectively. The phase boundary between the TI and BI is marked in dashed red line. Interestingly, it does not gap out after one breaks TRS. Instead it expands into

a double line (blue contour) with an IQHE phase with $\sigma_{xy} = \pm \frac{e^2}{h}$ appearing within. Metallic regions (grey regions) may also appear due to an indirect closing of the gap.

The gapless band touching lines in Fig. (2) do not disappear even as we further increase the TRS breaking terms. For $M_{\text{stg}} = 5t, 10t$ the eight-shaped contours in (2a) simply intersect the Δ axis further away (at $\Delta \approx \pm M_{\text{stg}}$) and gradually become squeezed along this axis. For large M_x , the closed contour in (2b) eventually splits along the δt axis and also intersect the Δ axis near $\pm M_x$. In addition some new band touching lines appear near the original line. This apparent robustness of the band touching lines will be explained in the next two sections.

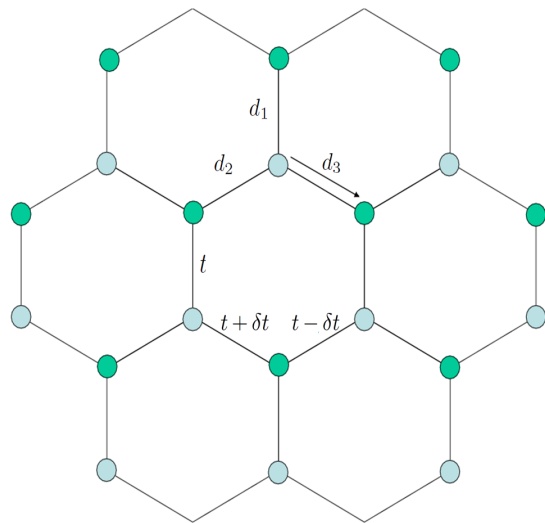


FIG. 1: Illustration of the lattice model and the different couplings given in Eq. (1)

III. WEAK TIME REVERSAL BREAKING

The low energy theory relevant for the vicinity of the transition from an ordinary to a topological band insulator in two dimensions consists of two Dirac modes dispersing around a pair of time reversed points K and K' in the Brillouin zone⁹. The effective hamiltonian for the massive Dirac fermions near one of these points is given by

$$H_K(k) = v_f \vec{k} \cdot \vec{\sigma}^\perp + m\sigma^z \quad (3)$$

where σ acts on the space of doubly degenerate states at K , \vec{k} measure the momenta relative to K and v_f is the Fermi velocity. The transition to the topological insulator is driven by changing the sign of the mass parameter m to a negative value. However we have freedom to vary another parameter that changes the separation between

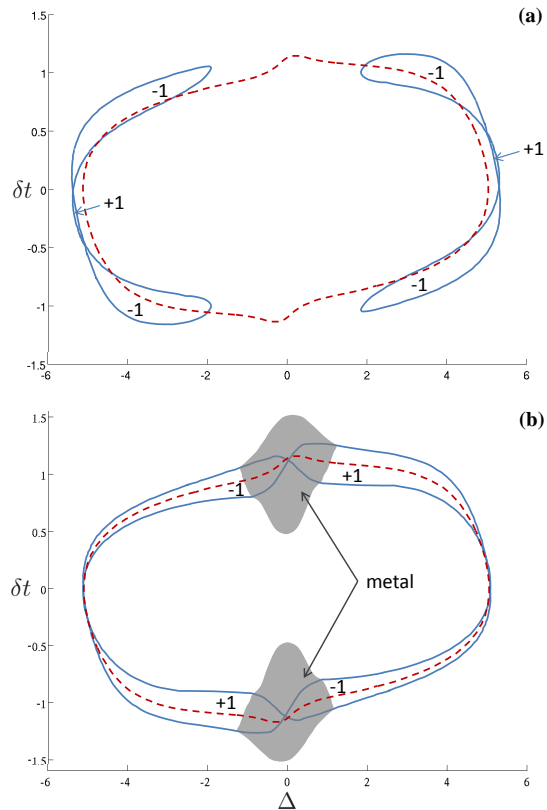


FIG. 2: Numerically obtained phase diagram of the model in Eqs. (1,2) as a function of a staggered potential (Δ) and staggered hopping (δt) in the presence of a staggered Zeeman field (a) or a uniform Zeeman field (b). With TRS the ordinary and topological band insulators are separated by a line of critical points (dashed red). When time reversal symmetry is broken this line can split and generically opens up into a Chern insulator phase of finite extent, having $\sigma_{xy} = \pm \frac{e^2}{h}$. Other parts of the phase boundary can open up to become metallic regions of finite extent as exemplified by the gray regions in panel (b). Notably, due to topological protection the gapless regions originating from the phase boundary persist to arbitrary large breaking of TRS.

K and K' while keeping $m = 0$. In the extended parameter space the transition is marked by a closed critical boundary surrounding the topological phase, as shown in Fig. (2a), dashed red line.

It will be useful to consider the mass formally as a third spatial coordinate k_z . Viewed in this way, Eq. (7) describes a massless Dirac cone in three dimensional space. The complete low energy theory including the two Dirac points in the extended parameter space is formally identical to a Weyl semi-metal¹⁰. In contrast to the gapless Dirac cones in two dimensional space the Dirac points in the extended three dimensional space (Weyl points) each carry a topological index that can be formulated as a Chern integer¹¹. This in particular protects the Dirac points in the extended three dimensional space from be-

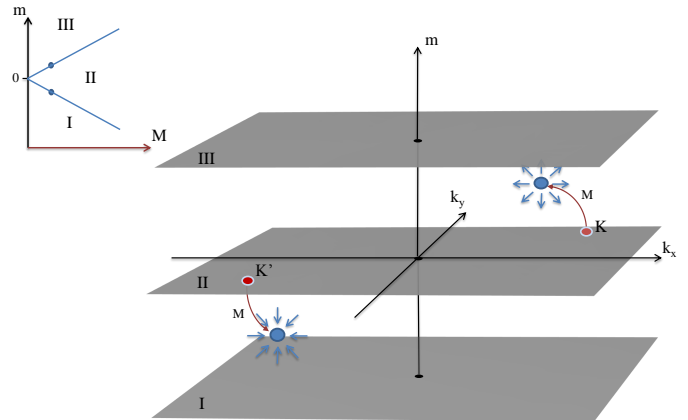


FIG. 3: Evolution of the Weyl points in the space (k_x, k_y, m) , where m is the tuning parameter, upon breaking of TRS with a field M . At non zero M the two Weyl points generically lie at different values of m . A system (II) with intermediate values of m is endowed with an integer Chern number from the two Weyl points.

ing gapped by perturbations that break time reversal symmetry as long as the K and K' points are spatially separated. Instead the consequence of such perturbations is to move these points away from the plane $m = 0$ (see Fig. 3). Moreover in absence of time reversal symmetry the Dirac points do not necessarily lie on the same m coordinate

The physical space of a single system however corresponds to a plane of constant m . When increasing the value of m with time reversal symmetry broken we generically pass two phase transitions as the plane crosses first one Dirac point and then the other. When the plane lies either above or below both Dirac points the topological flux emanating from them cancels and the system is topologically trivial. If on the other hand the physical plane is between the two Dirac points the topological flux adds up, endowing the system with a Chern number of $+1$ or -1 , depending on whether the Dirac cone with a positive Chern number is above or below the plane.

The above argument implies that a small TRS breaking perturbation opens the critical phase boundary into a Chern insulating phase. The extent of this phase initially grows with increasing TRS breaking field strength. At stronger fields the Chern insulator can eventually shrink and perhaps end altogether if the Dirac cones meet and annihilate each other. Finally we should note that the two Chern bands associated with the Chern insulator may also be separated by an indirect gap. In this case the Chern insulator would give way to a metal. This possibility is realized in certain parts of the phase diagram plotted in Fig. (2 b).

Before concluding this section we note that the generic

situation described above can be slightly modified in presence of various spurious symmetries. Let us give a few examples relevant to the model Hamiltonian (1). First in the case $\delta t = 0$ the operator product of time reversal (T), mirror with respect to the yz -plane and s_y is a symmetry of the Hamiltonian. As a result of this symmetry the two Dirac cones are constrained to remain on the same physical plane (m) even with broken TRS. For this reason the Chern insulating phases plotted in Fig. 2 are pinched at the points $\delta t = 0$. Similarly if we omit the extra spin orbit term λ_R then the product of T and s_z commutes with the Hamiltonian and prevents from the Chern insulator to open up at all. Furthermore, under these conditions ($\lambda_R = 0$) each of the critical points on the line $\Delta = 0$ (at $\delta t = \pm 1$) must have the Dirac points coincide $K = K'$. Then even an infinitesimal TRS breaking perturbation opens a gap for $\Delta = 0$ and therefore splits the phase boundary into two separated segments.

IV. TOPOLOGICAL STABILITY OF CRITICAL LINES

In the last section we discussed the perturbative stability of the phase boundary between the topological and ordinary insulator to weak TRS fields. However the numerical results of section (II) show that segments of the critical line persist to arbitrarily strong TRS breaking. We shall argue that this is due to topological protection that is much stronger than the perturbative stability discussed above.

The topological invariant is rather simple to formulate within the framework of the non interacting band theory. When TRS is broken, being on a critical line in the phase diagram is tantamount to having a single gapless Dirac cone located at some point \mathbf{K} in the Brillouin zone. If we go along the critical line in the two parameter phase diagram, closing a full loop parameterized by $\phi \in [0, 2\pi]$, the Dirac point charts at the same time a closed path $\mathbf{K}(\phi)$ in the two dimensional Brillouin zone. We can then associate with the critical line, as topological invariants, the two winding numbers of the loop on the toroidal Brillouin zone. Fig 4(a) and (c) show respectively examples of a topological and a non-topological loop. In the former case the critical line must persist in the phase diagram because the Brillouin-zone loop associated with it cannot be collapsed to a point no matter how strong the time reversal breaking field.

Our goal now is to relate the winding number on the Brillouin zone to a more fundamental topological invariant associated with quantized pumping. This will allow generalization to systems with disorder and interactions where the single particle Bloch wave-functions are not eigenstates. For this purpose we consider a closed path in the two parameter space $(\Delta, \delta t)$ that encircles the topological insulator from the out-side, that is a path $\gamma(\alpha)$ contained entirely in the ordinary gapped region, as de-

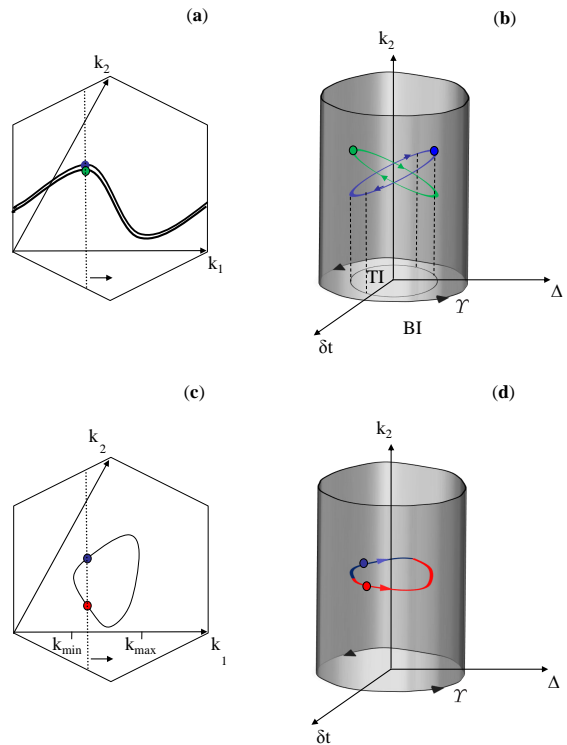


FIG. 4: The relation between windings in k -space and charge pumping. Panels (a) and (c) show the trajectory which the Weyl points make in the Brillouin zone if we move the system on the TI-BI phase boundary. Case (a) is an example with a topological winding number. Panels (b) and (d) show the respective trajectories of the Dirac points in the space $(\delta t, \Delta, k_2)$ for a fixed value of k_1 . The adiabatic path around the TI phase is extended to a distorted cylinder in that space. The charge pumped in such a cycle is given by the topological flux on the cylinder that originates from the Weyl points. This is ± 2 in case (b) and zero in case (d).

picted in Fig. (4 b). Let us now focus on the case where the two time reversed Dirac cones (on the phase boundary) wind in the k_1 direction of the Brillouin zone. By fixing k_1 we are dealing effectively with a one dimensional Hamiltonian, for which the pumped charge (along k_2) is related to an integer Chern number through the formula^{12,13}

$$C = \sum_n \int \frac{d\alpha dk_2}{\pi} \text{Im} \langle \partial_\alpha \psi_n | \partial_{k_2} \psi_n \rangle, \quad (4)$$

where $|\psi_n\rangle = |\psi_n(k_2, \alpha)\rangle$ is the wave function of the n -band at k_2 and α and the sum is over occupied bands. This is an integral over the surface of the cylinder-like surfaces shown in Fig. 4(b,d) that measures the amount of topological flux emanating from the Dirac points enclosed by it. These Dirac points can only reside on the TI-BI phase-boundary. But for a given value of k_1 we are not in general guaranteed to have any. For example, if the Dirac cones at K and K' chart paths in k -space that do not wind on the Brillouin zone (see e.g. Fig 4(c)),

then we can fix k_1 to a value such that the effective one dimensional Hamiltonian along k_2 is fully gapped, even on the phase boundary. On the other hand, if the Dirac cones at K and K' each winds around the Brillouin zone in the direction of k_1 then for any fixed value of k_1 we must have one Dirac point on the phase boundary originating from the trajectory of K and the other from K' .

The Dirac points originating from K and from K' contribute equal rather than opposite flux to the surface integral, contrary to what might have been naively guessed. To see this first recall that each Dirac point that is enclosed by our surface can be viewed as a hedgehog singularity in the relevant three dimensional space $\vec{\kappa} \equiv (k_2, \delta t, \Delta)$, with low energy hamiltonian near the Dirac point $H_{\mathbf{K},k_1}(\kappa) = -\delta\vec{\kappa} \cdot \vec{\sigma}$. The contribution of the Dirac point to the flux through the surface is the integer

$$C_{\mathbf{K},k_1} = \int \frac{d\theta d\phi}{4\pi} \hat{\kappa} \cdot \left(\frac{\partial \hat{\kappa}}{\partial \theta} \times \frac{\partial \hat{\kappa}}{\partial \phi} \right), \quad (5)$$

where $\hat{\kappa} = \vec{\delta\kappa}/|\delta\kappa|$. This is an integer that must remain fixed as a function of the continuous parameter k_1 . Let us then compare the flux $C_{\mathbf{K},k_1}$ emanating from the Dirac point at K to that from its time reversed partner $C_{\mathbf{K}',-k_1}$. Since in the Hamiltonian $-\delta\kappa \cdot \vec{\sigma}$ both k_1 and σ^y , and *only those*, change sign under time reversal symmetry the topological flux emanating from the two time reversed points is equal. Studying the winding number of the phase boundary between the TI and BI, we found it to be ± 1 along the direction of the staggered hopping. Therefore adiabatically changing the parameters of the model (1) to encircle the topological insulating phase, while staying in the ordinary insulator, entails pumping of exactly two electrons per row of the lattice. Such quantized pumping has been shown to be robust to disorder and interactions that invalidate the simple band picture¹³. We therefore expect the gapless phase boundaries to persist even in presence of interactions.

V. SUMMARY AND DISCUSSION

We showed that the critical phase boundaries separating a two dimensional topological insulator from an ordinary insulator are more robust to TRS breaking than the bulk phases themselves. First we established the perturbative stability of the critical lines in the generic case through a mapping to a Weyl metal in one higher dimension. A corollary of this analysis is that the critical phase boundary opens up into a Chern insulating phase or into a metallic phase with finite extent in the phase diagram. Next we formulated a criterion for yet stronger topological protection of the gapless phase boundaries that is insensitive to interactions and disorder. When the topological criterion holds the phase boundaries can split into segments, but the segments must persist to arbitrarily strong TRS breaking fields.

It is interesting to point out a surprising connection between the observations made here and previous work

on the ionic Hubbard model (i.e. Hubbard model supplemented by a staggered potential). The latter is used as a model to describe transitions between a band insulator and a correlated Mott insulator with increasing interaction strength. The onset of the Mott phase is typically defined through the emergence of magnetic order, both phases are however gapped to single particle excitations. A surprising and yet unexplained observation made in a number of numerical studies is that the magnetically ordered state itself is split into two regions separated by a metallic region with vanishing single particle gap¹⁴⁻¹⁶. Using a simple Hartree Fock description, the metallic phase can be seen to be smoothly connected to a phase boundary between a TI and ordinary band insulator at zero magnetization and non-vanishing spin orbit coupling (see App. A). The persistence of the metallic phase deep into the magnetically ordered state, even without spin orbit, is due to the topological robustness of the phase boundary.

Finally, as an extension to this work it would be interesting to classify the robustness of phase boundaries between topological and ordinary insulators in higher dimensions (as well as higher dimensional parameter spaces). This can be done using the general classification of defects and pumps in such phases^{17,18}.

Appendix A: Protected gapless regions in the ionic Hubbard model

In this appendix we relate the metallic regions that appear inside the magnetically ordered phase of the ionic Hubbard model^{14-16,19} with the persistent phase boundaries discussed in the main text of this paper. The ionic Hubbard model is defined by the following Hamiltonian on a square lattice

$$H_{\text{el}} = \sum_{\langle ij \rangle, s} t c_{i,s}^\dagger c_{j,s} + \sum_{i,s} \Delta \xi_i n_{i,s} \quad (A1)$$

$$+ \sum_i U (n_{i,\uparrow} - 1/2)(n_{i,\downarrow} - 1/2),$$

where $c_{i,s}$ annihilates an electron with spin s on the i 'th site, $\xi_i = \pm 1$ denotes an alternating sign on the two sublattices and $n_{i,s}$ is the occupancy.

The qualitative features of this model can be seen from a Hartree Fock (HF) analysis. The interaction term is decoupled assuming a staggered magnetic moment

$$\sum_i U (n_{i,\uparrow} - 1/2)(n_{i,\downarrow} - 1/2) \approx -\frac{1}{2} \sum_i M_{stg} \xi_i c_{i,s}^\dagger \sigma_{s,s'}^x c_{i,s'}, \quad (A2)$$

and the resulting quadratic Hamiltonian is solved together with the self consistency condition²⁰

$$\vec{M}_i = \frac{U}{2} \langle c_{i,s}^\dagger \vec{\sigma}_{s,s'} c_{j,s'} \rangle_{\vec{M}}. \quad (A3)$$

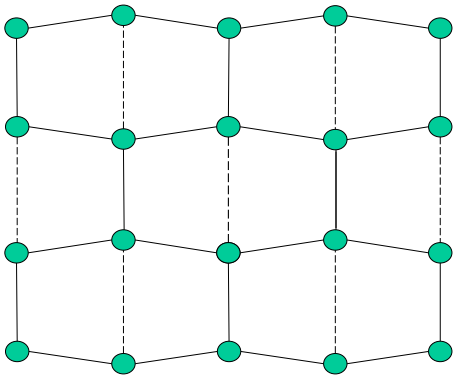


FIG. 5: A square lattice can be viewed as a deformed hexagonal lattice with one extra bond per side (dashed line).

The mean field theory shows a second order transition into the (AF) magnetically ordered state at a critical interaction strength $U_c \propto t/\ln(t/\Delta)$. The single particle excitation spectrum of the mean field Hamiltonian is given by

$$E_{k,s} = \pm \sqrt{\epsilon_k^2 + (sM_{stg} + \Delta)^2}, \quad (\text{A4})$$

$$\epsilon_k = 2t(\cos(k_x a) + \cos(k_y a)),$$

where s denotes the spin along the x -direction. Notably as the magnetization increases it eventually reaches the value $|M_{stg}| = |\Delta|$. At this point the excitation gap for spins with $s = -\text{sign}(\Delta/M_{stg})$ closes and a gapless point appears.

We argue that the gapless point inside the magnetically ordered phase can be related to the critical point between a TI and BI in presence of TRS. To this end we add the following perturbation which gradually deforms the free part of ionic Hubbard model on the square lattice into the Kane and Mele model defined on a honeycomb lattice²¹

$$V = i\lambda \sum_{\langle\langle ij \rangle\rangle, s_z} \nu_{ij} s_z c_{is_z}^\dagger c_{js_z}, \quad (\text{A5})$$

$$- \lambda \sum_{\langle ij \rangle_v, s_z} c_{is_z}^\dagger c_{js_z}.$$

Here $\langle\langle ij \rangle\rangle$ denotes pairs of sites connected by two nearest neighbor bonds which do not include the dashed-bond in Fig. (5) and $\langle ij \rangle_v$ denotes sites sharing a dashed-bond. The spectrum of the mean-field Hamiltonian together with the addition V is given by

$$E_{k,s} = \pm \sqrt{|\epsilon_k|^2 + (sA + \Delta)^2}, \quad (\text{A6})$$

$$\epsilon_k = 2te^{ik_y a}(\cos(k_x a) + \cos(k_y a)) - \lambda e^{2ik_y a},$$

$$A = \sqrt{4\lambda^2[\sin(2k_x a) - 2\cos(k_y a)\sin(k_x a)]^2 + M_{stg}^2},$$

where $s = \pm 1$ now denotes the spin projection along the direction $(M_{stg}, 0, 2\lambda[\sin(2k_x a) - 2\cos(k_y a)\sin(k_x a)])$.

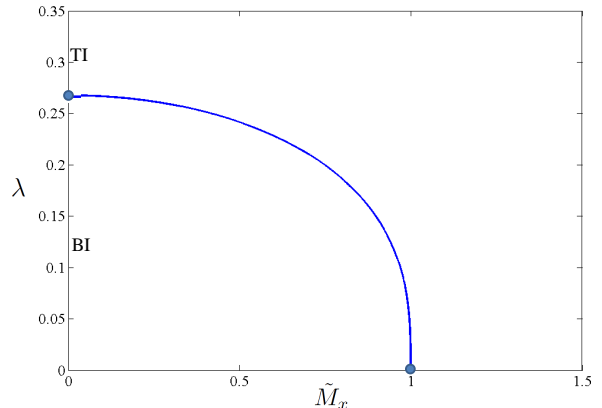


FIG. 6: Regions with gapless charge excitations in the ionic Hubbard model at $t = \Delta = 1$ as a function of the spontaneous magnetization M_{stg} and the spin-orbit perturbation λ (see Eqs. (A1,A2,A5)). The $\lambda = 0$ axis corresponds to the usual ionic Hubbard model where a gapless point appears for $M_{stg} = \Delta$. Increasing λ at $M_{stg} = 0$ another gapless point appears marking the transition between a BI phase and a TI phase. Interestingly, these two points are smoothly connected implying that the former one could be seen as part of the protected gapless surface discussed in the main text.

Using Eq. (A6) we obtain the equations for the critical points where the gap closes:

$$4\lambda^2[\sin(2k_x a) - 2\sin(k_x a)]^2 = \Delta^2 - M_{stg}^2, \quad (\text{A7})$$

$$\cos(k_x a) = \left(\frac{\lambda}{2t} - 1\right).$$

These equations give a critical line in the space λ versus M_{stg} which is shown in Fig. 6. The critical line extends all the way to the axes at $\lambda = 0$ corresponding to the ionic Hubbard model on the square lattice. Thus the gapless point in the magnetically ordered phase of the ionic Hubbard model can be understood as persistence of the critical surface separating the TI and BI phases due to the topological protection discussed in the main text.

-
- ¹ C. L. Kane and E. J. Mele, Phys. Rev. Lett. **95**, 146802 (2005).
- ² B. A. Bernevig, T. L. Hughes, and S.-C. Zhang, Science **314**, 1757 (2006), <http://www.sciencemag.org/content/314/5806/1757.full.pdf>, URL <http://www.sciencemag.org/content/314/5806/1757.abstract>.
- ³ M. König, S. Wiedmann, C. Brüne, A. Roth, H. Buhmann, L. W. Molenkamp, X.-L. Qi, and S.-C. Zhang, Science **318**, 766 (2007).
- ⁴ D. Hsieh, D. Qian, L. Wray, Y. Xia, Y. S. Hor, R. J. Cava, and M. Z. Hasan, Nature **452**, 970 (2008).
- ⁵ C. Brüne, C. X. Liu, E. G. Novik, E. M. Hankiewicz, H. Buhmann, Y. L. Chen, X. L. Qi, Z. X. Shen, S. C. Zhang, and L. W. Molenkamp, Phys. Rev. Lett. **106**, 126803 (2011), URL <http://link.aps.org/doi/10.1103/PhysRevLett.106.126803>.
- ⁶ E. Berg, M. Levin, and E. Altman, Phys. Rev. Lett. **106**, 110405 (2011).
- ⁷ This term is included to remove a coincidental symmetry along the $\Delta = 0$ line consisting of TRS times inversion times S_z . This symmetry causes a metallic region to appear between the BI and TI and makes our analysis slightly more cumbersome. Also note that such a term will arise if the deformation of the hopping generates an in-plane electric field.
- ⁸ S. Rachel and K. Le Hur, Phys. Rev. B **82**, 075106 (2010), URL <http://link.aps.org/doi/10.1103/PhysRevB.82.075106>.
- ⁹ S. Murakami, S. Iso, Y. Avishai, M. Onoda, and N. Nagaosa, Phys. Rev. B **76**, 205304 (2007), URL <http://link.aps.org/doi/10.1103/PhysRevB.76.205304>.
- ¹⁰ X. Wan, A. M. Turner, A. Vishwanath, and S. Y. Savrasov, Phys. Rev. B **83**, 205101 (2011), URL <http://link.aps.org/doi/10.1103/PhysRevB.83.205101>.
- ¹¹ M. V. Berry, Proceedings of the Royal Society of London. Series A, Mathematical and Physical Sciences **392**, pp. 45 (1984), ISSN 00804630, URL <http://www.jstor.org/stable/2397741>.
- ¹² D. J. Thouless, Phys. Rev. B **27**, 6083 (1983).
- ¹³ Q. Niu, D. J. Thouless, and Y.-S. Wu, Phys. Rev. B **31**, 3372 (1985).
- ¹⁴ A. Garg, H. R. Krishnamurthy, and M. Randeria, Phys. Rev. Lett. **97**, 046403 (2006).
- ¹⁵ K. Bouadim, N. Paris, F. Hébert, G. G. Batrouni, and R. T. Scalettar, Phys. Rev. B **76**, 085112 (2007).
- ¹⁶ N. Paris, K. Bouadim, F. Hébert, G. G. Batrouni, and R. T. Scalettar, Phys. Rev. Lett. **98**, 046403 (2007).
- ¹⁷ R. Roy, ArXiv e-prints (2011), 1104.1979.
- ¹⁸ J. C. Y. Teo and C. L. Kane, Phys. Rev. B **82**, 115120 (2010), URL <http://link.aps.org/doi/10.1103/PhysRevB.82.115120>.
- ¹⁹ S. S. Kancharla and E. Dagotto, Phys. Rev. Lett. **98**, 016402 (2007).
- ²⁰ For simplicity we ignored the density terms generated by the decoupling since these could be absorbed into Δ and the Chemical potential.
- ²¹ C. L. Kane and E. J. Mele, Phys. Rev. Lett. **95**, 146802 (2005).